Solar Energy Materials & Solar Cells 98 (2012) 357–362

Contents lists available at SciVerse ScienceDirect

Solar Energy Materials & Solar Cells

journal homepage: www.elsevier.com/locate/solmat

A simple and low-cost technique for silicon nanowire arrays based solar cells

Bohr-Ran Huang [a,*], Ying-Kan Yang [a], Tzu-Ching Lin [a], Wen-Luh Yang [b]

[a] Graduate Institute of Electro-Optical Engineering and Department of Electronic Engineering, National Taiwan University of Science and Technology, Taipei 106, Taiwan, ROC
[b] Department of Electronic Engineering, Feng Chia University, Taichung 407, Taiwan, ROC

ARTICLE INFO

Article history:
Received 29 April 2011
Received in revised form
14 November 2011
Accepted 17 November 2011
Available online 7 December 2011

Keywords:
Silicon nanowire (SiNW) arrays
Phosphorus silicate glasses (PSG)
Solar cells

ABSTRACT

A new PSG doping process was developed using a sol-gel method with phosphorus pentoxide (P_2O_5) powder combined with a screen-printing technique for the fabrication of electrodes. This process was applied in silicon nanowire (SiNW) arrays based solar cells. The PSG-doped SiNW arrays were used as both the anti-reflectance layer and the n^+ emitter for the solar cells. The morphology and photoelectric characteristics of the SiNW array solar cells were measured by a scanning electron microscope (SEM), a UV/VIS/NIR spectrophotometer, a quantum efficiency measurement system and a solar cell simulator. It was found that the reflectivity (R_λ), internal quantum efficiency (IQE), series resistance (R_s) and power conversion efficiency (PCE) were influenced by the aspect ratio and the density of the PSG-doped SiNW arrays. Results indicate that there is a competition phenomenon between the aspect ratio and the density. It was observed that certain aspect ratio (~5.15) with appropriate density (~34.5%) of PSG-doped straight-aligned SiNW arrays possessed better solar cell (~10.15%) performance. The SiNW array solar cells showed potential for low cost and mass-production in commercial solar cells applications.

1. Introduction

In the past few years, silicon nanostructure-based solar cells such as nanorods, nanocorns, nanotips, and nanowires have attracted much interest because of their novel chemical and physical properties [1–4]. The use of silicon nanowires (SiNWs) in solar cells was particularly interesting [5–8]. The SiNW arrays demonstrated broadband optical absorption because of multiple scattering incidents causing strong light trapping properties. SiNW arrays can be used as solar cell absorbers [9–11]. Recently, several methods have been reported for synthesizing SiNWs, including chemical vapor deposition (CVD) [8], laser ablation [12], physical vapor deposition (PVD) [13,14], etc. Among these, wet electroless etching [15–17], reactive ion etching (RIE) [18,19], and electrochemical etching [20] have been widely used as an alternative top-down route in the cell fabrication process. In this process, the n^+ emitter formation step uses phosphorus oxychloride ($POCl_3$) as the dopant source [15,17,19], but this is corrosive, toxic and expensive. Most other studies deposited both the front and rear electrodes using the sputtering and/or evaporation system [15,16,18–20]. By contrast, the new doping source of the PSG solution and the screen-printing method are convenient and cost-effective. However, the main challenge facing SiNW based solar cells is the loose contact between the electrodes and the SiNWs. Several research groups have tried to overcome this problem through slanting aligned SiNW array solar cells [6] and selective SiNW array solar cells [16].

This study proposes a low-cost SiNW arrays fabrication process using a new PSG solution as the doping source, with a screen-printing method to coat electrodes to create SiNW arrays based solar cells. Solar cell parameters including V_{oc}, J_{sc}, FF, PCE, and R_s are studied, along with structural and morphological appearance.

2. Experimental details

SiNW arrays were synthesized on a p-type (1–10 Ω cm, B doped, 520 μm), Cz silicon (100) wafer using the wet electroless etching technique [21]. First, the wafer was cleaned ultrasonically in acetone and isopropyl alcohol for 20 min in each cleaning solution. Second, the cleaned silicon wafer was immersed in a mixture of 5 mol/L hydrofluoric acid (HF) aqueous and 0.02 mol/L silver nitrate ($AgNO_3$) solution for different time durations (1–20 min) at room temperature. Following the wet electroless etching process, the silicon wafer was wrapped with a thick silver film consisting of high-density tree-like dendritic structures [21]. To remove the capped silver, the as-prepared samples were dipped into a 30 wt% HNO_3 aqueous solution for 60 s. Finally, the samples were rinsed with deionized water and blown dry in air.

The PSG solution was prepared by the sol-gel method, mixing P_2O_5 powder, ethanol (C_2H_5OH), tetraethoxysilane (TEOS) and

* Corresponding author. Tel.: +886 2 27333141x3273; fax: +886 2 27376424.
E-mail address: huangbr@mail.ntust.edu.tw (B.-R. Huang).

0927-0248/$ - see front matter © 2011 Elsevier B.V. All rights reserved.
doi:10.1016/j.solmat.2011.11.031

deionized water followed by a spin coating process on the SiNW arrays. For solar cells fabrication, the PSG/SiNW samples were heated at 850 °C for 10 min to form the PSG-doped SiNW array (as the n^+ emitter layer) and parasitic layer. Based on the secondary ion mass spectroscopy (SIMS) measurement, the emitter layer has a peak doping level of 2.1×10^{21} cm^{-3}. Typically, the doping profile results in an junction depth $X_J \sim 0.83$ μm with a background doping level of $\sim 1 \times 10^{16}$ cm^{-3} as the length of PSG-doped SiNW arrays is 279 nm. The parasitic layer was then removed by 60 s immersion in a HF aqueous solution. Following the phosphorus diffusion process, the front silver (Ag) grid electrode was formed by the screen-printing technique and the rear layer was coated by Al paste. The samples were then followed by a co-firing process in N_2 ambient at 720 °C for 10 min to form the back surface field (BSF). The schematic diagrams for the fabrication of the SiNW array based solar cells are presented in Fig. 1.

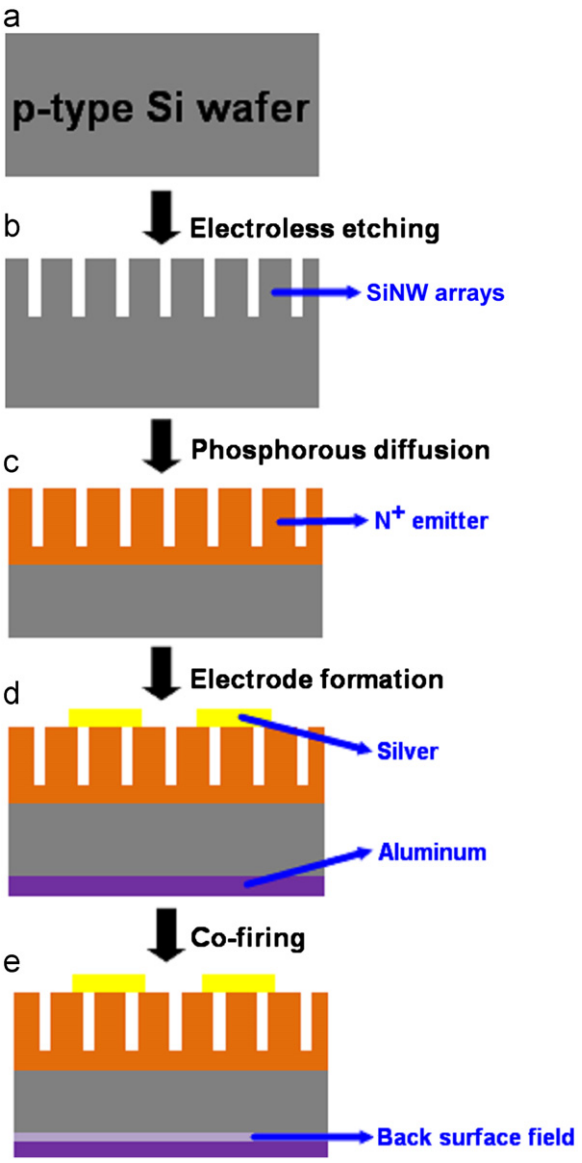

Fig. 1. Schematic illustration of the fabrication process for preparing SiNW arrays based solar cells: (a) Initial p-type silicon wafer. (b) Fabrication of the SiNW arrays. (c) Formation of PSG-doped SiNW arrays(n-type SiNW emitters). (d) Al layer and the silver front grid electrodes are coated on the rear and front surfaces of the PSG-doped SiNW arrays, respectively. (e) Co-firing of metal electrodes to form back surface field.

The morphologies of the SiNW array solar cells were examined by field emission scanning electron microscopy (FESEM, JEOL JSM–6700 F, operated at 15 kV). The densities of the PSG-doped SiNW arrays were calculated using the image analysis software (SigmaScan, SPSS, Chicago, IL). Optical reflectance spectra measurements in the 300–1100 nm wavelength range were performed with a UV/VIS/NIR Spectrophotometer (Jasco V-670). All samples were electrically tested under standard test conditions (STC, air mass 1.5 irradiation, $T=300$ K, $P=100$ mW/cm^2). One sun of light intensity was calibrated against a reference cell made by Newport, traceable to the National Renewable Energy Laboratory (NREL). The quantum efficiency spectra were measured using a monochromator and chopped-light system made by Newport.

3. Results and discussion

Fig. 2 shows the surface morphology images of the initial SiNW arrays with 1 and 2 min wet electroless etching. Despite the short etching time, SiNW array structures can be seen. Fig. 3 shows the tilted top-region SEM images of the PSG-doped SiNW arrays with different etching time durations (1–20 min). Fig. 3(a) shows a PSG-doped SiNW arrays with short etching time resulted in a porous surface morphology. Fig. 3(c) shows the length and diameter of the PSG-doped SiNW arrays shrank (from ~200 nm to ~91 nm) and increased (from ~33 nm to ~46 nm) in comparison with the SiNW array. This was caused by the high temperature PSG doping process (850 °C) and the removal of the parasitic layer including the oxide and PSG layer. This suggests a simultaneous combination of phosphorous diffusion and oxidation processes taking place in the PSG/SiNWs interface during the PSG doping process. The SiNW arrays were further fused together following the PSG doping process to form the PSG-doped SiNW arrays. The parasitic layer was then removed by the HF solution treatment. Similarly, this phenomenon is also observed and discussed below in terms of the longer etching times.

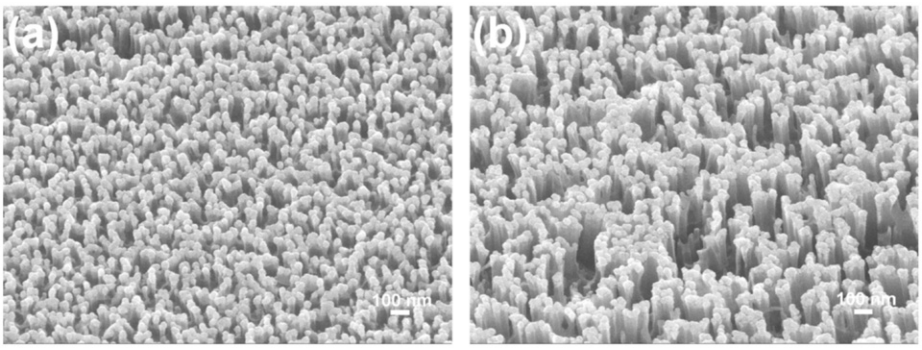

Fig. 2. Typical SiNW array planar images using the electroless etching technique prior to the PSG doping process with different length of (a) 100 nm and (b) 200 nm.

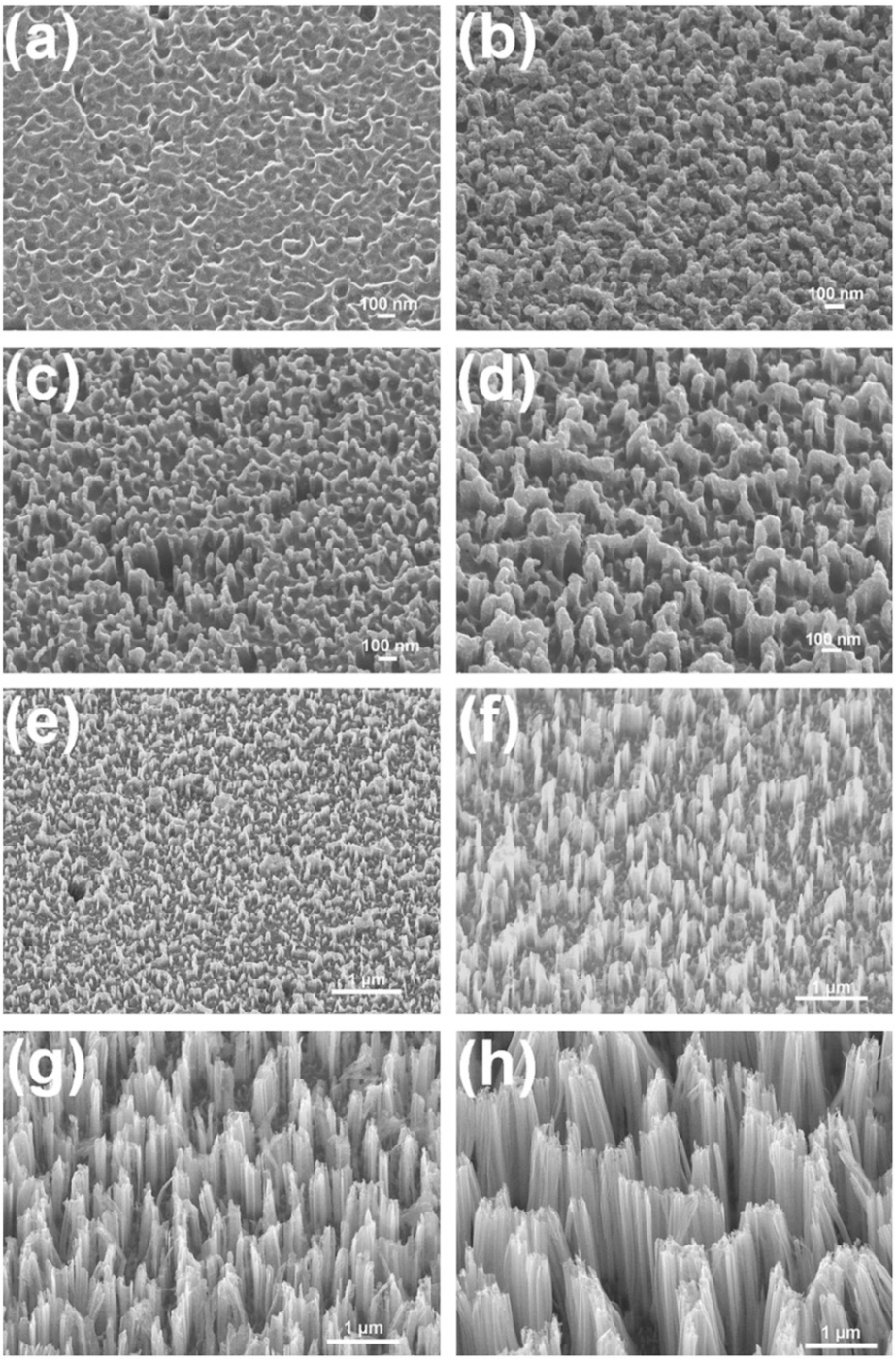

Fig. 3. PSG-doped SiNW array planar images with different length: (a) porous, (b) 60 nm, (c) 91 nm, (d) 279 nm, (e) 312 nm, (f) 544 nm, (g) 1100 nm and (h) 2934 nm.

Fig. 3(b)–(e) show the morphologies of PSG-doped SiNW arrays were straight-aligned structures. As the etching time was increased to 20 min, the samples behaved more like the bundled SiNW structures shown in Fig. 3(f), (g), and (h). The formation of these bundled SiNW arrays can be attributed to the surface tension forces exerted on the nanowires during drying of the samples [22]. In addition, the density of the SiNW array decreased from ~45.3% to ~24.3% as the etching time increased, which is consistent with the results of several other studies [23]. Table 1 summarizes the lengths, diameter and aspect ratio of all samples, which increase with electroless etching time. This indicates that the density of the PSG-doped SiNW arrays decreased as the etching time increased because of the bundled SiNW structure. However, the density of the SiNW array was further decreased following the PSG doping process is noteworthy.

Fig. 4 reveals the reflectivity spectra measurements of PSG-doped SiNW arrays with different length. As observed, the R_λ of the porous structure was ~34.1%. The R_λ decreased from ~25.6% to ~3.1% as the length of PSG-doped SiNW arrays increased. PSG-doped SiNW arrays with longer length possessed better antireflection properties. This suggests that there are three important factors in producing good antireflection properties in SiNW arrays: (1) extremely high surface area for the greater length of the SiNW arrays, (2) a surface nanostructure of the SiNW arrays corresponding to the subwavelength-structured (SWS) surface, and (3) a gradual change in the refractive index with the increase

Table 1
Extracted length, diameter, aspect ratio, density, reflectance of PSG-doped SiNW array with various etching time.

Electroless etching time (*min*)	Length of PSG-doped SiNW arrays (nm)	Diameter (nm)	Aspect ratio (A. R.)	Density (%)	Reflectivity (%)
1	0	–	–	–	~34.1
1.5	~60	50	1.2	45.3	~25.6
2	~91	46	1.97	37.8	~23.8
2.5	~279	54	5.15	35.7	~21.3
3	~312	50	6.24	33.5	~20.1
6	~544	58	9.38	31.2	~5.2
10	~1100	75	14.67	27.8	~3.5
20	~2934	83	35.35	24.3	~3.1

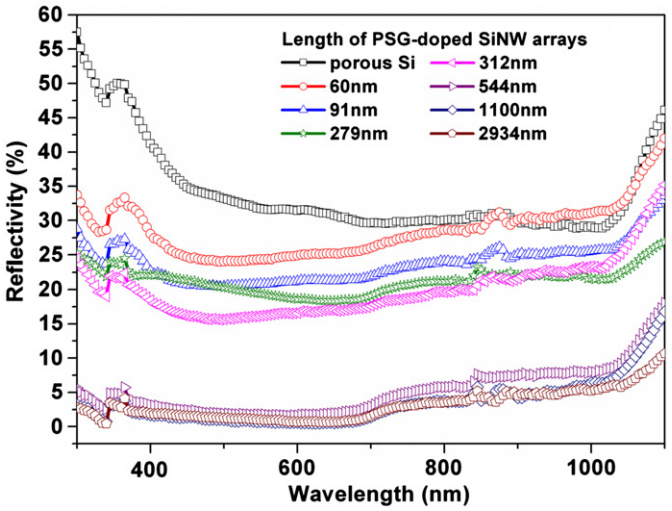

Fig. 4. Optical reflectivity spectra of PSG-doped SiNW array solar cells with different length.

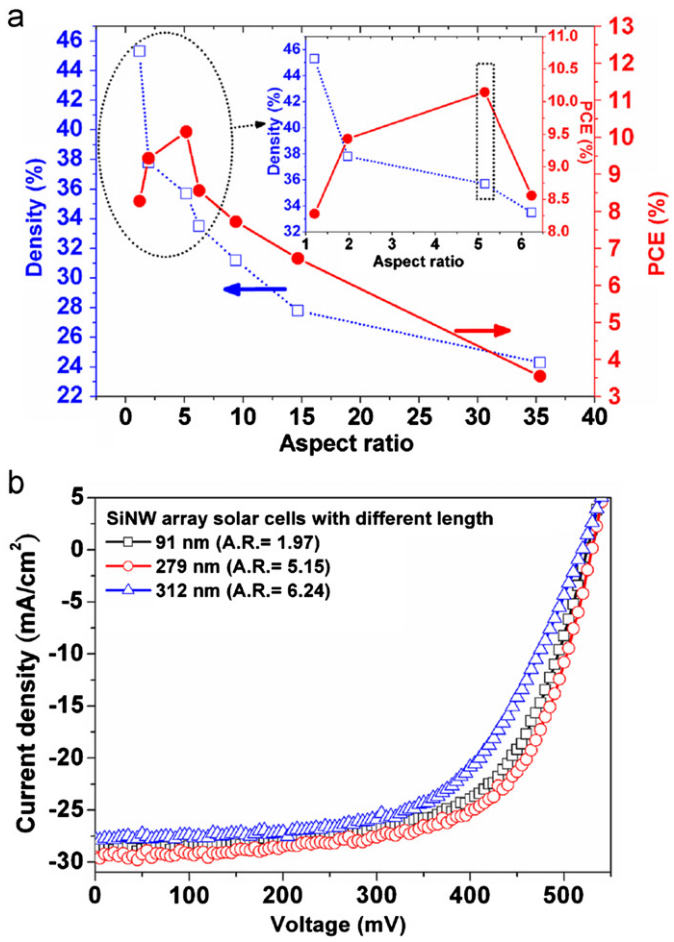

Fig. 5. (a) Density and power conversion efficiency for SiNW array solar cells with different aspect ratio. The inset shows density and power conversion efficiency for SiNW array solar cells with aspect ratio between 1 and 6.5. (b) Photovoltaic I–V curves for SiNW array solar cells for different length of 91 nm, 279 nm and 312 nm.

on the depth of the SiNW arrays that closely resembles a multi-antireflection layer coating [25,27,28]. The reflectivities of all samples are also summarized in Table 1.

Fig. 5(a) shows the density and PCE for SiNW array solar cells with different aspect ratios. As shown in the inset of Fig. 5(a), it was observed that the PCE decreases when the aspect ratio is smaller or larger than 5.15, indicating competition between the aspect ratio and the density of the PSG-doped SiNWs. That is, there is an optimal condition between the aspect ratio and the density of the PSG-doped SiNWs. It was observed that a certain aspect ratio (~5.15) with an appropriate density (~34.5%) of PSG-doped straight-aligned SiNW arrays exhibited improved solar cell (~10.15%) performance. Similar results were also reported by S.-H. Baek's group, which achieved an improved PCE performance of 7.1% for silicon wire solar cells with an aspect ratio of 6.1 [20]. Nonetheless, the vertically-aligned Si wire arrays were fabricated by electrochemical etching and the p-n junction was prepared by the spin-on-dopant (SOD) diffusion method [20].

Fig. 5(b) shows the photovoltaic current density versus voltage measurements for the SiNW array solar cells with different length of 91, 279, and 312 nm, respectively. The corresponding electrical parameters for different length of SiNW array solar cells are summarized in Table 2.

Fig. 6 shows the PCE, along with the R_s for the SiNW array solar cells with different length. The R_s value was calculated by the corrected light and dark IV-curve comparison method [24]:

$$R_s = \frac{V_{dark,mpp} - V_{light,mpp} - (|J_{sc}| - |J_{mpp}|)R_{s,dark}}{|J_{mpp}|},$$

where $R_{s,dark}$ represents the series resistance, which was calculated by

$$R_s = \frac{V_{dark,Jsc} - V_{oc}}{|J_{sc}|},$$

The R_s of the SiNW array solar cells is found to increase from 1.17 to 8.88 Ω as the length increases. This suggests poor electrical contacts during the longer length of the SiNW array solar cells due to the higher aspect ratio (>5.15) and lower density ($<35.7\%$), which might be discontinuous between the front electrode and the PSG-doped SiNW arrays. As shown in Tables 1 and 2, the bundled PSG-doped SiNW array structure exhibits a higher R_s than that of the PSG-doped straight-aligned SiNW array structure. The lower R_s value in solar cells will lead to a smaller electrical loss and promote solar cell performance. Moreover, the length of the PSG-doped SiNW arrays also has a strong effect in cell performance because the minority carrier lifetime will decrease as the length increase [25,26]. This indicates that straight-aligned SiNW array structure-based solar cell possesses better photovoltaic characteristics than the porous structure and the bundled structure.

Fig. 7 shows the IQE spectra derived from the external quantum efficiency (EQE) following: IQE=EQE/(1–R_λ). The IQE of the porous structure solar cell is higher than that of SiNW array solar cells and the IQEs decrease as the length increases. There is a noticeable reduction of IQE at short wavelengths for the length of

Table 2
Illuminated I–V measurements of SiNW array solar cells under STC.

Length of SiNW array Solar cell (nm)	V_{oc} (mV)	J_{sc} (mA/cm^2)	FF (%)	PCE (%)	R_s (Ω)	R_{sh} (Ω)
0	507.5 ± 2.50	26.15 ± 3.25	57.4 ± 6.10	7.51 ± 0.10	2.91 ± 0.66	371 ± 231
~60	505.0 ± 5.00	25 ± 0.50	65.5 ± 0.2	8.28 ± 0.06	1.17 ± 0.10	565 ± 188
~91	522.5 ± 2.50	27.95 ± 0.65	64.45 ± 0.45	9.43 ± 0.20	2.02 ± 0.32	390 ± 46
~279	520 ± 10.00	30.65 ± 1.15	4.85 ± 0.35	10.15 ± 0.05	1.36 ± 0.40	446 ± 64
~312	522.5 ± 2.50	28.65 ± 0.85	57.25 ± 2.45	8.56 ± 0.09	3.76 ± 0.25	405 ± 110
~544	520 ± 0.05	24.8 ± 0.50	59.8 ± 1.10	7.72 ± 0.32	3.95 ± 0.08	511 ± 60
~1100	525 ± 5.00	21.3 ± 0.20	56.89 ± 3.02	6.37 ± 0.34	7.78 ± 0.18	1019 ± 775
~2934	492.5 ± 7.50	13.9 ± 3.10	53.45 ± 6.75	3.55 ± 0.31	8.88 ± 0.08	486 ± 333

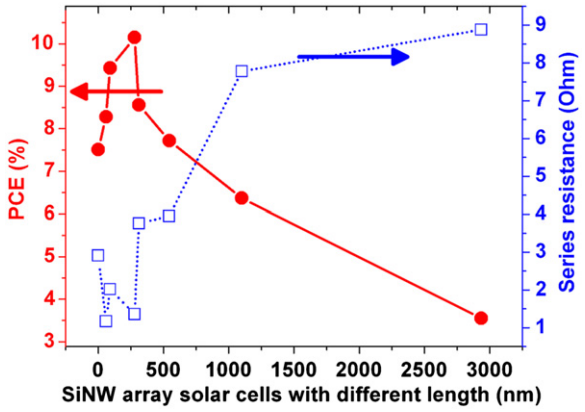

Fig. 6. Power conversion efficiency and series resistance for SiNW array solar cells with different length.

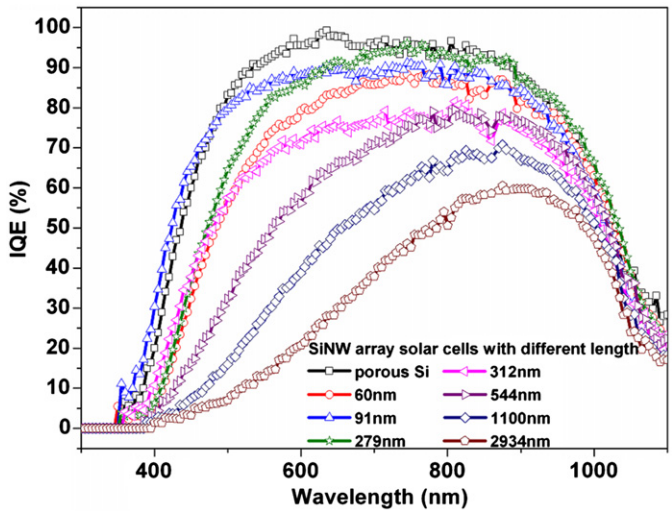

Fig. 7. Internal quantum efficiency spectra of SiNW array solar cells with different length.

SiNW array solar cells over 544 nm. This shows that longer length exhibited a greater surface recombination loss phenomenon due to the larger surface area [8,19]. The IQEs for the longer length of the SiNW array solar cells are improved at long wavelengths, which suggest that longer length have good absorption properties at long wavelengths via the diffraction mechanism [15].

However, the poor electrical contact, reduction of the minority carrier lifetime, and loss of the surface recombination for lower density and longer length of SiNW array solar cells would reduce the PCE. Competition phenomenon exists between the aspect ratio and the density of SiNW arrays indicating that a specific aspect ratio with an appropriate density of the straight-aligned SiNW array structure solar cell is critical for achieving better solar cell performance.

In this study, a PCE of ~10.15% is achieved for SiNW array based solar cells. The PCE is comparable to those featured in previous reports (9.24%–11.1%) [16–18]. Combined with a screen-printing technique, this new PSG solution exhibited reasonable potential for low cost solar cell applications. However, the correlation between the aspect ratio, the density and the PCE needs to be investigated further. Moreover, the PCE might be further improved by optimizing the front and rear electrode contacts, and by improving the doping techniques and the selective patterned nanostructures for the SiNW arrays.

4. Conclusion

This study presents a simple approach combining a new low cost PSG dopant solution and a screen-printing technique to fabricate the n^+ emitter and the electrodes for SiNW array based solar cells. It is found that the aspect ratio and the density for SiNW array solar cells performance are in competition, and the straight-aligned SiNW array structures with a certain aspect ratio(~5.15) and an appropriate density (35.7%) possesses better solar cell performance. Superior photovoltaic characteristics for the PCE (~10.15%) with a J_{sc} of 30.65 mA/cm^2 and a V_{oc} of 520 mV are achieved. These results could be applied to the potential application in low-cost and high efficiency SiNW based solar cells.

Acknowledgment

This work was partially supported by the National Science Council of Taiwan under grant no. 100-2221-E-011-052-MY3.

References

[1] E.C. Garnett, P. Yang, Silicon nanowire radial p-n junction solar cells, Journal of the American Chemical Society 130 (2008) 9224–9225.
[2] E.C. Cho, S. Park, X. Hao, D. Song, G. Conibeer, S.C. Park, M.A. Green, Silicon quantum dot/crystalline silicon solar cells, Nanotechnology 19 (2008) 245201/1–245201/5.
[3] X.J. Hao, E.C. Cho, G. Scardera, Y.S. Shen, E.B. Amalric, D. Bellet, G. Conibeer, M.A. Green, Phosphorus-dopedilicon quantum dots for all-silicon quantum dot tandem solar cells, Solar Energy Materials & Solar Cells 93 (2009) 1524–1530.
[4] H.C. Yuan, V.E. Yost, M.R. Page, P. Stradins, D.L. Meier, H.M. Branz, Efficient black silicon solar cell with a density-graded nanoporous surface: optical properties, performance limitations, and design rules, Applied Physics Letters 95 (2009) 123501/1–123501/3.
[5] B. Tian, X. Zheng, T.J. Kempa, Y. Fang, N. Yu, G. Yu, J. Huang, C.M. Lieber, Coaxial silicon nanowires as solar cells and nanoelectronic power sources, Nature 449 (2007) 885–890.
[6] H. Fang, X. Li, S. Song, Y. Xu, J. Zhu, Fabrication of slantingly-aligned silicon nanowire arrays for solar cell applications, Nanotechnology 19 (2008) 255703/1–255703/6.

[7] V. Sivakov, G. Andra, A. Gawlik, A. Berger, J. Plentz, F. Falk, S.H. Christiansen, Silicon nanowire-based solar cells on glass: synthesis, optical properties, and cell parameters, Nano Letters 9 (2009) 1549–1554.
[8] O. Gunawan, S. Guha, Characteristics of vapor-liquid-solid grown silicon nanowire solar cells, Solar Energy Materials & Solar Cells 93 (2009) 1388–1393.
[9] L. Hu, G. Chen, Analysis of optical absorption in silicon nanowire arrays for photovoltaic applications, Nano Letters 7 (2007) 3249–3252.
[10] L. Tsakalakos, J. Balch, J. Fronheiser, M.Y. Shih, S.F. LeBoeuf, M. Pietrzykowski, P.J. Codella, B.A. Korevaar, O. Sulima, J. Rand, A. Davuluru, U. Rapol, Strong broadband optical absorption in silicon nanowire films, Journal of Nanophotonics 1 (2007) 013552/1–013552/10.
[11] A.I. Hochbaum, P. Yang, Semiconductor nanowires for energy conversion, Chemical Reviews 110 (2010) 527–546.
[12] A.M. Morales, C.M. Lieber, A laser ablation method for the synthesis of crystalline semiconductor nanowires, Science 279 (1998) 208–211.
[13] L. Schubert, P. Werner, N.D. Zakharov, G. Gerth, F.M. Kolb, L. Long, U. Gösele, T.Y. Tan, Silicon nanowhiskers grown on 〈111〉 Si substrates by molecular-beam epitaxy, Applied Physics Letters 84 (2004) 4968–4970.
[14] V. Sivakov, F. Heyroth, F. Falk, G. Andrä, S. Christiansen, Silicon nanowire growth by electron beam evaporation: Kinetic and energetic contributions to the growth morphology, Journal of Crystal Growth 300 (2007) 288–293.
[15] D. Kumar, S.K. Srivastava, P.K. Singh, M. Husain, V. Kumar, Fabrication of silicon nanowire arrays based solar cell with improved performance, Solar Energy Materials and Solar Cells 95 (2011) 215–218.
[16] X. Li, J. Li, T. Chen, B.K. Tay, J. Wang, H. Yu, Periodically aligned Si nanopillar arrays as efficient antireflection layer for solar cell applications, Nanoscale Research Letters 5 (2010) 1721–1726.
[17] H. Li, R. Jia, C. Chen, Z. Xing, W. Ding, Y. Meng, D. Wu, X. Liu, T. Ye, Influence of nanowires length on performance of crystalline silicon solar cell, Applied Physics Letters 98 (2011) 151116/1–151116/3.
[18] Y. Cheng, Z. Gang, L.D. Young, L.H. Min, L.Y. Dae, Y.W. Jong, P.Y. Jun, K.J. Min, Self-assembled wire arrays and ITO contacts for silicon nanowire solar cell applications, Chinese Physics Letters 28 (2011) 035202/1–035202/3.
[19] O. Gunawan, K. Wang, B. Fallahazad, Y. Zhang, E. Tutuc, S. Guha, High performance wire-array silicon solar cells, Progress in Photovoltaics: Research and Applications 19 (2011) 307–312.
[20] S.H. Baek, H.S. Jang, J.H. Kim, Characterization of optical absorption and photovoltaic properties of silicon wire solar cells with different aspect ratio, Current Applied Physics 11 (2011) S30–S33.
[21] T. Qiu, P.K. Chu, Self-selective electroless plating: An approach for fabrication of functional 1D nanomaterials, Materials Science and Engineering R 61 (2008) 59–77.
[22] K. Zhu, T.B. Vinzant, N.R. Neale, A.J. Frank, Removing structural disorder from oriented TiO2 nanotube arrays reducing the dimensionality of transport and recombination in dye-sensitized solar cells, Nano Letters 7 (2007) 3739–3746.
[23] K. Peng, Y. Wu, H. Fang, X. Zhong, Y. Xu, J. Zhu, Uniform, axial-orientation alignment of one-dimensional single-crystal silicon nanostructure arrays, Angewandte Chemie International Edition 44 (2005) 2737–2742.
[24] D. Pysch, A. Mette, S.W. Glunz, A review and comparison of different methods to determine the series resistance of solar cells, Solar Energy Materials and Solar Cells 91 (2007) 1698–1706.
[25] K. Peng, Y. Xu, Y. Wu, Y. Yan, S.T. Lee, J. Zhu, Aligned single-crystalline Si nanowire arrays for photovoltaic applications, Small 1 (2005) 1062–1067.
[26] S.C. Shiu, S.B. Lin, S.C. Hung, C.F. Lin, Influence of pre-surface treatment on the morphology of silicon nanowires fabricated by metal-assisted etching, Applied Surface Science 257 (2011) 1829–1834.
[27] Y. Kanamori, M. Sasaki, K. Hane, Broadband antireflection gratings fabricated upon silicon substrates, Optics Letters 24 (1999) 1422–1424.
[28] C.C. Striemera, P.M. Fauchet, Dynamic etching of silicon for broadband antireflection applications, Applied Physics Letters 81 (2002) 2980–2982.